Journal of Applied Polymer Science

Compatibilizing Effect of Halloysite Nanotubes in Polar–Nonpolar Hybrid System

Parthajit Pal, Mrinal Kanti Kundu, Asish Malas, Chapal Kumar Das
Materials Science Centre, Indian Institute of Technology Kharagpur, Kharagpur, India
Correspondence to: P. Pal (E - mail: pal.p85@gmail.com)

ABSTRACT: This article explores the effect of halloysite nanotubes (HNTs) and modified HNTs (M-HNTs) on the properties of immiscible blend system based on polar polyoxymethylene (POM) and nonpolar polypropylene (PP) polymers. HNTs have been modified by *N*-(*β*-aminoethyl)-*γ*-aminopropyltrimethoxysilane (APTMS). Modification is confirmed by Fourier transform infrared spectroscopy (FTIR), also FTIR confirms the interaction between polymer blend and HNTs/M-HNTs. Morphology of the nanocomposites are demonstrated by scanning electron microscope (SEM) and dispersion of HNTs/M-HNTs are observed by transmission electron microscope (TEM). In nanocomposites, average dispersed domain sizes reduce in the presence of HNTs/M-HNTs but significant reduction has been observed in the case of M-HNT-filled nanocomposites rather than unmodified HNT-filled nanocomposites. The M-HNT acts as a reinforcing agent as well as bridging tool in polar–nonpolar hybrid system. Modification of HNTs brings compatibility in between the blend partners and reveals improved dynamic mechanical, thermal, and tensile properties than that of the pure blend system. © 2013 Wiley Periodicals, Inc. J. Appl. Polym. Sci. **2014**, *131*, 39587.

KEYWORDS: blends; compatibilization; composites; clay; mechanical properties

Received 9 December 2012; accepted 23 May 2013
DOI: 10.1002/app.39587

INTRODUCTION

Polymer blending is the mixture of two or more different polymers at a certain ratio. Advantages of polymer blends are enhancement of engineering resins performance, improvement of specific properties, and achievement of desired set of properties in between two or more polymers at lower cost, easier formulation, high productivity, and so on. Miscible blend of two polymers exhibit intermediate properties of the two unblended polymers. Most of the polymer blends are immiscible in nature; to overcome this, compatibilizers are generally used to increase the interfacial adhesion between the immiscible polymers.[1,2]

Naturally occurring aluminosilicate with molecular formula of $Al_2Si_2O_5(OH)_4.nH_2O$ is known as halloysite nanotubes (HNTs). It has the similar geometry with carbon nanotubes (CNTs). HNTs are tubular in structure and the size of its tubules varies from 500 to 1000 nm in length and from 15 to 100 nm in inner diameter.[3–5] HNTs are low-cost clay material and in recent days these are used as nanofillers in polymer nanocomposites because of their unique structure and properties.[6–8] Polar polyoxymethylene (POM) and nonpolar polypropylene (PP) both polymers are crystalline in nature, they do not differ much more in melting temperature, so their processing temperature is almost same.[9–13]

In this article, we have chosen POM and PP polymers and tried to fabricate a polar–nonpolar hybrid material. Li and Shimizu[14] reported that in the presence of 5 wt % organoclay co-continuous structure formed in 50/50 w/w poly(phenyleneoxide) (PPO)/polyamide 6 (PA6) blend. In our research work, we have found that 1 : 1 ratio of POM–PP blend shows the matrix-droplet morphology. Our aim is to achieve compatibility in between two polymers by incorporation of HNTs/modified HNTs (M-HNTs). The present study is based on the development of POM–PP–HNT nanocomposites and the effect of HNTs/M-HNTs on the blend system.

EXPERIMENTAL

Materials

POM was supplied by BASF (Germany), of grade H2320 004. PP of grade H030SG purchased from Reliance industries limited, India. HNTs were obtained as nanopowder from Sigma-Aldrich (Germany). Its surface area is 64 m^2/g, pore volume of 1.25 mL/g, and specific gravity of 2.53 g/cm^3. *N*-(*β*-aminoethyl)-*γ*-aminopropyltrimethoxysilane (APTMS) (DAW Corning, Z6020, silane; DAW Corning Corporation Midland, MI) was used as received without further purification.

Modification of HNTs

At first, 3 mL of APTMS dissolved in 80 mL of dry toluene (toluene made dry by using sodium bisulphate) in combination with 1.0 g of the dry HNTs (HNTs baked at 400°C for 2 h in a

furnace) and the suspension dispersed ultrasonically for 20 min. The suspension was refluxed at 100°C for 24 h. It was filtered and rinsed for several times with fresh toluene to remove excess APTMS, and then dried at 80°C under vacuum overnight.[15,16]

Preparation of Blend and Nanocomposites

Fifty-by-fifty weight per weight ratio of POM–PP pure blend (named as B) was prepared via melt mixing process using internal melt mixer (40 rpm) at 190°C. In this pure blend system, 1 wt % pure HNTs and 1 wt % of M-HNTs were added separately to prepare unmodified HNT nanocomposite (B-HNT) and M-HNT nanocomposite (B-MHNT).

CHARACTERIZATIONS

FTIR Study

In order to verify the interfacial interaction, samples were tested with the Tensor 27 (Bruker, Germany) Fourier transform infrared spectroscopy (FTIR) equipment in humidity-free atmosphere at room temperature in transmission mode. Spectra were taken from 4000 to 400 cm^{-1}. For the powdered sample, pellets were made from mixture of powder sample and KBr at the weight ratios of 1 : 200. For polymeric nanocomposites, thin films were prepared by using compression molding machine.

Surface Morphology Study

The tensile fractured surfaces of specimens were coated with a thin layer of gold for conductivity and the surface morphology of the specimens were examined under high vacuum with an acceleration voltage of 20 kV in a JEOL JSM-5900 LV for scanning electron microscope (SEM) experiment. Elemental mapping and energy dispersive X-ray analysis (EDAX) were also done with the same instrument. The particle size analysis gives number average domain diameter (D_n), which was calculated with Scion Image analyzer software (Scion Corp., USA).

TEM Analysis

Powdered HNTs/M-HNTs and its extent of dispersion in the nanocomposites (300 nm) were studied by transmission electron microscope (TEM): JEM-2100, JEOL; operating at an accelerating voltage of 200 kV.

Dynamic Mechanical Thermal Analysis

Dynamic mechanical thermal analysis (DMTA) of pure blend and nanocomposites were done by a TA Instrument (DMA 2980 model) in single cantilever bending mode. The storage modulus (E′) and tan δ were recorded at the frequency of 1 Hz from –80°C to 140°C temperature and at a heating rate of 5°C /min. Experiment were conducted under nitrogen purging.

Thermogravimetric Analysis

Thermogravimetric analysis (TGA) was investigated using TGA-209F thermal analyzer, (manufactured by NETZSCH Germany) from 30°C to 600°C at a heating rate of 10°C /min under nitrogen atmosphere.

Tensile Property

Tensile test was carried out by using Hounsfield HS 10 KS (universal testing machine) with a gauge length of 35 mm and crosshead speed of 1 mm/min at room temperature. Four specimens of each sample were tested and averages of the results were recorded.

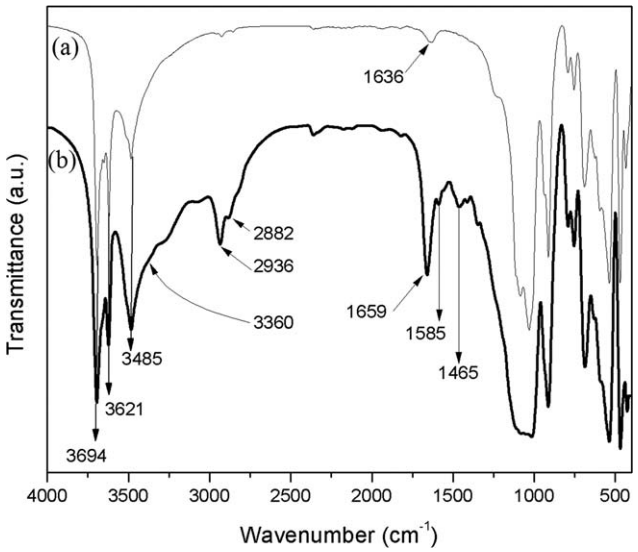

Figure 1. FTIR graphs of (a) pure HNTs and (b) M-HNTs.

RESULTS AND DISCUSSION

FTIR Study

Figure 1 displays the FTIR spectra of M-HNTs and pure HNTs for comparison. This speculation is in accord with the previous reports on halloysite- and APTMS-grafted silica materials.[16] In Figure 1, absorption at 3694, 3621, and 3485 cm^{-1} arise because of inner surface hydroxyl group, inner hydroxyl group stretching of HNTs, and hydroxyl group stretching of water, respectively. Absorption peak at 3360 cm^{-1} comes because of N–H asymmetric stretching for M-HNTs, but it was absent the in case of pure HNTs. M-HNT also shows asymmetric and symmetric C–H stretching at 2936 and 2882 cm^{-1}, respectively.

The deformation of O–H stretching of water comes at 1659 and 1636 cm^{-1}, the N–H deformation comes at 1585 cm^{-1}, and C–H deformation at 1465 cm^{-1}. These results suggest that APTMS successfully anchored on the halloysite surface.[15,16]

Figure 2 displays the FTIR curve of pure HNTs, pure blend (B), and nanocomposites (B-HNT and B-MHNT). In Figure 2(c) curve shows the sudden decrease in transmittance percentage of –OH group of HNTs, which clearly demonstrates the physical interaction that took place between the –OH group and the polymer blend.[17] The other peaks of the blend and nanocomposites at around ~2985 cm^{-1} and (1459–1374 cm^{-1}) were because of C–H stretching and C–H bending mode of vibrations, respectively.

Surface Morphology Study

The SEM micrographs of pure blend (B) and nanocomposites are shown in Figure 3(a–c); the micrograph of pure blend shows the immiscibility and matrix-droplet morphology. To confirm which polymer formed droplets in B blend, we have done elemental mapping which is shown in Figure 4(a–c). In the SEM image of B [Figure 4(a)] area under the white box was mapped. Red color indicated the presence of carbon atoms [Figure 4(b)] and the green color indicated the presence of oxygen atoms [Figure 4(c)]. As POM consist of oxygen atoms, hence it

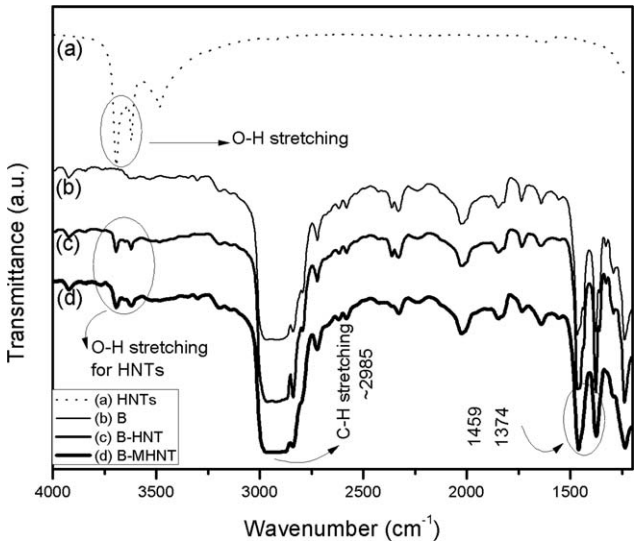

Figure 2. FTIR graph of (a) pure HNTs, (b) B, (c) B-HNTs, and (d) B-MHNTs.

is easy to say from this image mapping that POM exists as droplets and PP goes to the matrix phase in blend system.

Now it can be observed from Figure 3(a) that the average domain size in noncompatibilized binary blend is larger when compared to the other domain size of nanocomposites (evident from Table I). Mainly, HNTs restrict the small droplets to agglomerate themselves and M-HNTs do the same job with better extent, hence droplets remain smaller in size as they were.[18] Larger domain size in pure binary blend might be because of the weak adhesion between the two polymers. The holes in the micrographs of the binary blend system were formed because of the domain pullout.

Figure 3(b) shows that after addition of HNTs the spherical domains of POM get deformed to ellipsoid shapes. The domain size of POM notably decreased after addition of M-HNTs [Figure 3(c)]. It was believed that polar–polar interaction took place between HNTs and POM as POM has polar C–O backbone,[11] and HNTs contain polar hydroxyl (–OH) groups, and hence it may be inferred that most of the HNTs are going into the POM phase. Thus, at the time of melt blending there was a competition in between POM and PP to acquire HNTs and during this time of mutual pulling, POM domains might have forcefully dragged the HNTs from PP matrix which led to the deformation of spherical POM domains to ellipsoidal shapes.[19] For better understanding about the dispersion behavior of natural clays, SEM images with high magnification are shown in Figure 5(a–c). Figure 5(a) of pure blend shows that the matrix surface is very smooth in the absence of HNTs. Figure 5(b) showed that HNTs go into POM as well as PP phase (more evident from EDAX values, Figure 6). Figure 5(c) displayed that the M-HNTs are bridged in between two polymers and concurrently surface roughness of the matrix occurred. The long organic chains which were acquired by M-HNTs can entangle with PP chains; and the roughness of the matrix surface which was observed in B-MHNT nanocomposite could be because of that chain interlocking. The bridging effect because of this chain anchoring between the M-HNTs and PP can improve the stress transformation from one phase to other and hence it can be suggested that more energy will be required to separate the droplets from the matrix in B-MHNT nanocomposite. Nayak et al.[18] described that modified multiwalled CNT brings better mechanical properties on PPO/LCP blend system. Y. Ye et al.[20] showed that the impact strength of the epoxy resin filled with HNTs was enhanced because of nanotube bridging in the composite. They suggested that HNTs are the potential alternative to the expensive CNTs for nanocomposite fabrication. M. Liu et al.[21] also reported about the bridging concept at the interface for the epoxy/HNT composites and observed improved performance and morphological characteristics of the hybrid.

To confirm about the distribution of HNTs in B-HNT nanocomposite, EDAX had been studied as shown in Figure 6 (a and b). The elements present in matrix phase and in droplet phase are shown in Figure 6(a and b), respectively. Both of the figures informed that Al and Si elements were present in the matrix as well as in the domain phase which states about the presence of HNTs in both phases.

TEM Analysis

TEM images of pure HNTs and M-HNTs are given in Figure 7. It was clear from Figure 7(b) that when the modifiers get stacked onto the wall of the HNTs, the average diameter increased.

TEM images of nanocomposites are presented in Figure 8(a–c). For B-HNT nanocomposite [Figure 8(a)] it can be seen that agglomeration occurred because of poor interaction between HNTs and polymer blend, also Van der Waals force of attraction might have played a role for the agglomeration. But for the B-MHNT nanocomposites, M-HNTs were finely dispersed in the polymer matrices which may be because of the better

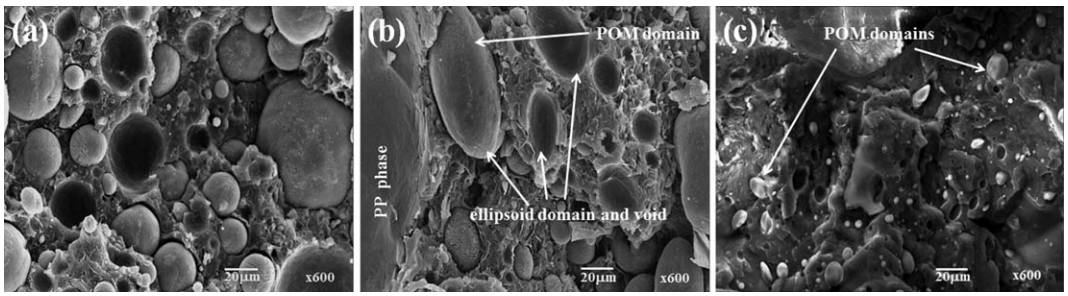

Figure 3. SEM micrograph of (a) pure polymer blend, (b) B and nanocomposites, (c) B-HNTs, and (d) B-MHNTs.

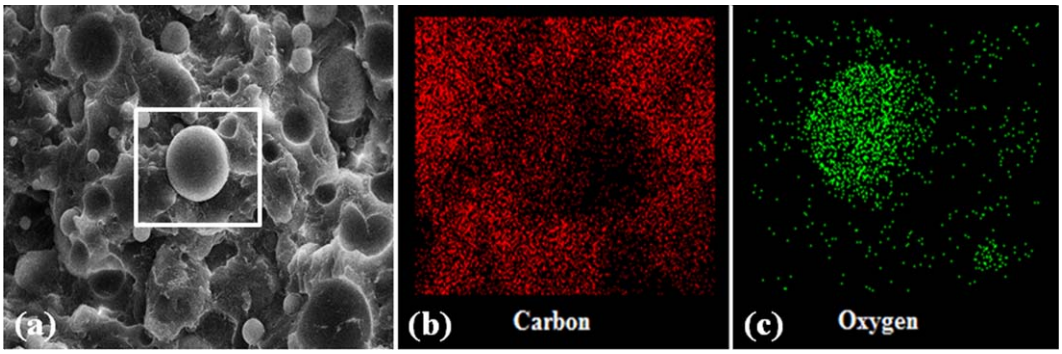

Figure 4. Elemental mapping of carbon and oxygen of pure blend (B). [Color figure can be viewed in the online issue, which is available at wileyonlinelibrary.com.]

interaction between modified clay (M-HNTs) and POM–PP blend. S. Bose et al.[22] suggested that clay modification can enhance the interaction parameter between the two blend system. M-HNTs achieved long organophilic chains after modification, resulting in better interaction between M-HNTs and immiscible polymer blend system. Figure 8(c) showed that M-HNTs remain in between two phases which states about its compatibilization.

DMTA Analysis

By this analysis, the viscoelastic property of pure polymers, pure blend, and nanocomposites were measured as a function of temperature. In Figure 9(i), the storage modulus curve of pure polymers (PP and POM), pure blend (B), and nanocomposites (B-HNT and B-MHNT) are displayed. Samples were studied at glassy and rubbery region in between temperature ranges from –80°C to 140°C . It was clear from Figure 9(i) that B-MHNT nanocomposites have the highest storage modulus (E′) as compared to the others. The higher values of storage modulus of nanocomposites compared to pure blend indicate the reinforcing effect of halloysite. Better dispersion of M-HNTs enhanced the higher polymer–matrix interaction area and thus increased the storage modulus.

From the tan δ plot in Figure 9(ii), we get the glass-transition temperatures (T_g) of the analyzed samples. The T_g and the corresponding tan δ values of pure polymers, pure blend, and the nanocomposites are recorded in Table II. Here, B showed the lowest T_g value at 11°C, but for B-HNT and B-MHNT nanocomposite it was 12°C and 14°C, respectively. Here, the nanotubular clays restrict the movement of the polymer chains which was the reason behind the improvement of T_g with the incorporation of pure and modified HNTs in the blend system.[23]

Table I. Particle Size Analysis

Sample code	D_n (μm)
B	33.7
B-HNTs	22.8
B-MHNTs	11.9

TGA Analysis

TGA plot for pure polymers (PP and POM), pure blend (B), and B-HNT/B-MHNT nanocomposites are shown in Figure 10, and the corresponding temperatures at 5% weight loss are also displayed in the same figure. All the curves showed the single step degradation. From Figure 10 it can be said that PP was highly thermally stable and POM was the least thermally stable polymer. Five percent degradation took place at 259°C for virgin polymer blend B, but the degradation temperature increases with the addition of HNTs. It reaches up to 263°C for B-HNT and further increases on incorporation of M-HNTs. Thus, B-MHNT showed 5% weight loss at 270°C, which was because of the good interaction between the blend and the M-HNTs. Hence, it can be inferred that the thermal degradation has

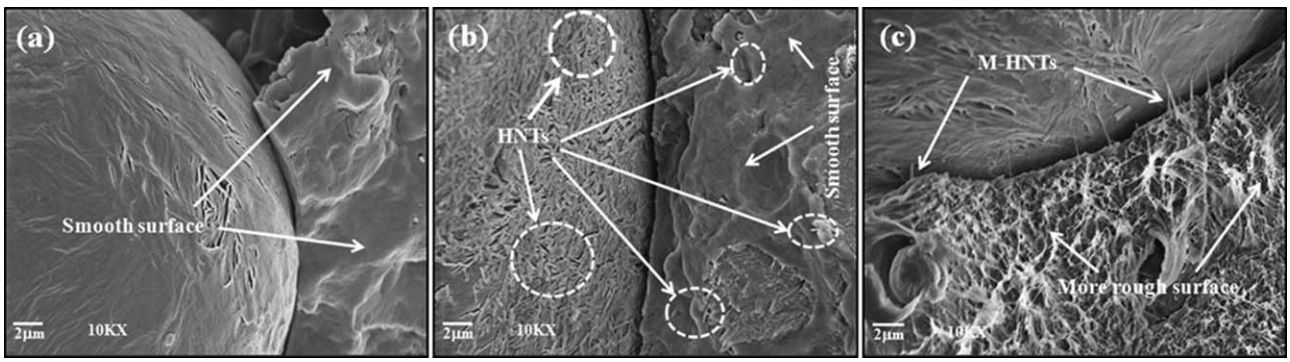

Figure 5. High magnification SEM of (a) pure polymer blend, (b) B and nanocomposites, (c) B-HNTs, and (d) B-MHNTs.

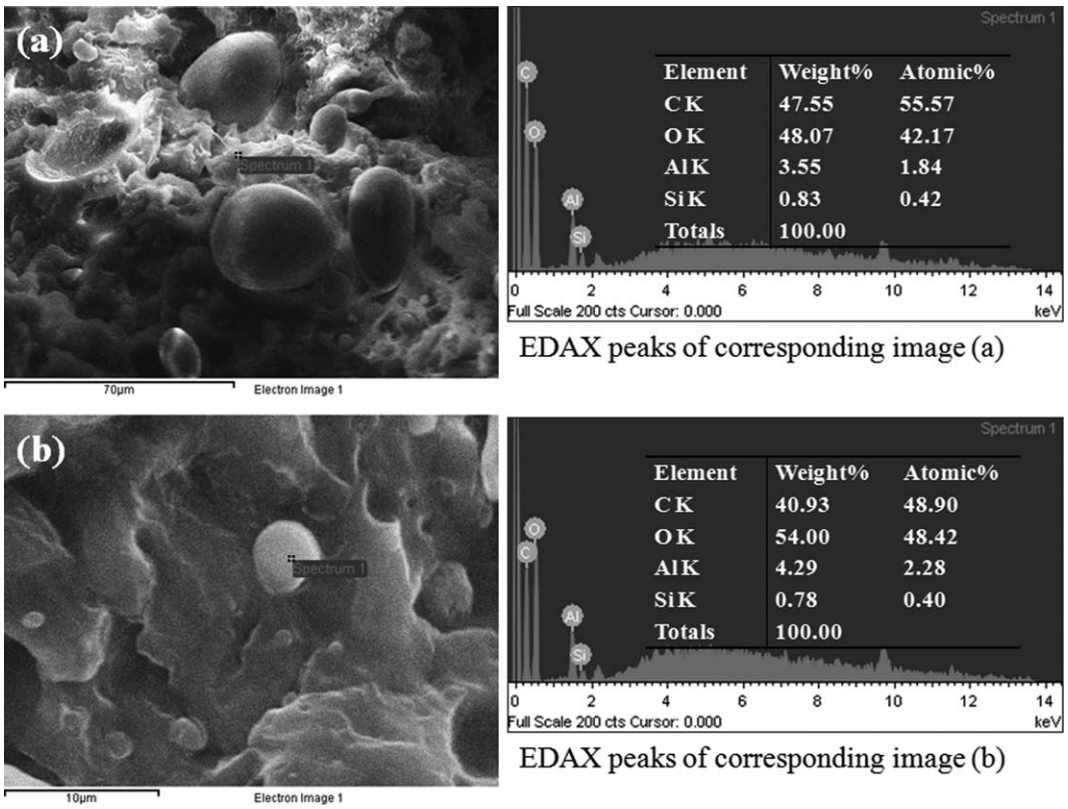

Figure 6. EDAX of B-HNT nanocomposite (a) peaks on matrix phase and (b) peaks on droplet phase.

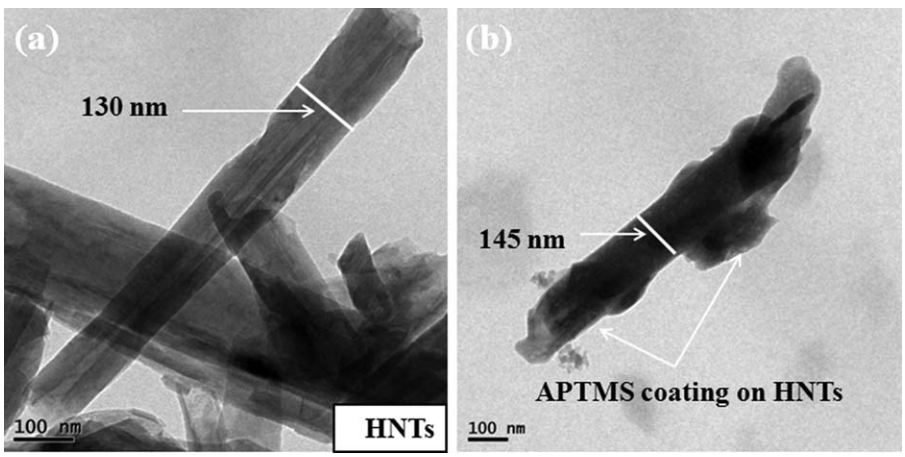

Figure 7. TEM images of (a) pure HNTs and (b) M-HNTs.

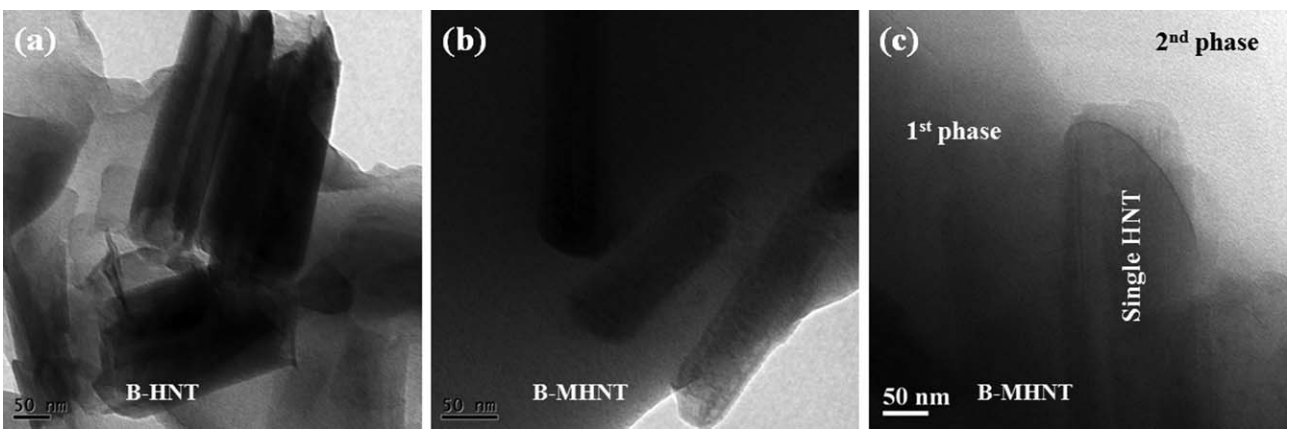

Figure 8. TEM images of (a) B-HNTs and (b,c) B-MHNTs.

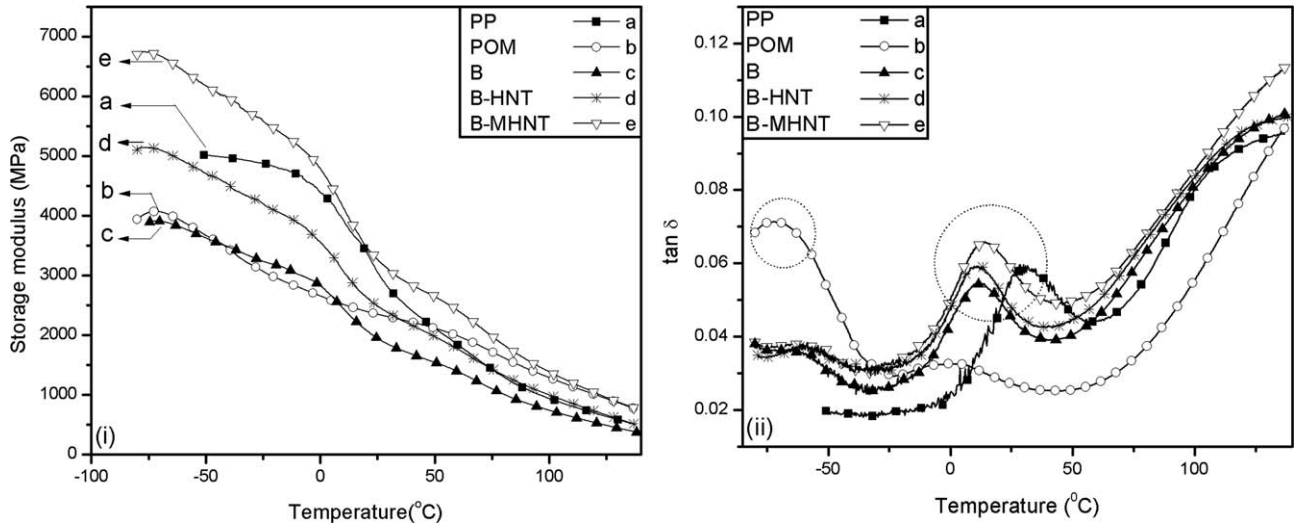

Figure 9. (i) Storage modulus and (ii) tan δ curves of (a) PP, (b) POM, (c) B, (d) B-HNTs, and (e) B-MHNTs.

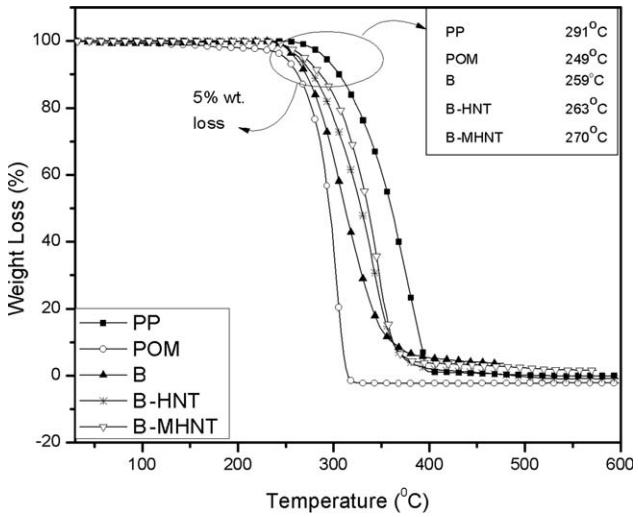

Figure 10. TGA curves of PP, POM, B, B-HNTs, and B-MHNTs.

enhanced because of the barrier properties of the HNTs. Previous researchers also proposed about the barrier properties of nanofillers that were responsible for increased thermal stability of respective nanocomposites.[24–27]

Table II. Glass-Transition Temperature (T_g) and Tan δ of Pure Polymers, Pure Blend (B), and HNT/M-HNT Nanocomposites

Sample code	T_g (°C)	Tan δ at peak
POM	−72	0.059
PP	30	0.071
B	11	0.054
B-HNTs	12	0.058
B-MHNTs	14	0.065

Tensile Property

Variations in tensile properties of pure blend along with the nanocomposites are summarized in Table III. Improvement of tensile strength was observed in the case of HNT-/M-HNT-loaded nanocomposites as compared to pure blend. For the M-HNT-based nanocomposites, tensile strength was more pronounced because of the better dispersion and bridging effect of M-HNTs at the POM–PP interface (shown in surface morphology study). Applied stress was transferred from the polymer matrix to the fillers, and hence tensile properties of the composites are higher than the pure blend. Elongation at break decreases from pure blend to B-MHNT nanocomposites which ascribes the enhancement of rigidity.[23]

CONCLUSIONS

Modification of HNTs was done by APTMS and confirmed by FTIR analysis. The dispersion of M-HNTs in blend matrix was better as compared to unmodified one. The dynamic mechanical strength, thermal stability, and tensile strength of the nanocomposite were profoundly improved with the incorporation of M-HNTs into the blend system. Reduction in the number average particle size of the dispersed phase was observed in the presence of HNT-/M-HNT-loaded nanocomposites. For B-MHNT nanocomposite, the domain size of POM was remarkably decreased after the addition of 1 wt % M-HNTs, which indicates that M-HNTs improve the interfacial interaction

Table III. Tensile Properties of Blend and Nanocomposites

Sample code	Tensile strength (MPa) [±2]	Elongation at break (%) [±0.2]	Tensile modulus (MPa) [±10]
B	39	9.38	1859
B-HNTs	40	9.27	1957
B-MHNTs	46	9.18	2193

between the matrix phase and the dispersed phase, resulting in the improvement of compatibility in between the blend partners. All these significant improvements in the overall properties of the M-HNT-filled nanocomposites indicate the synergistic effect of M-HNTs as a compatibilizer between the two immiscible polymers.

REFERENCES

1. Utracki, L. A.; Polymer Blends Handbook; Kluwear Academic Publishers: Amsterdam, The Netherlands, **2002**. vol. *1*.
2. Harrats, C.; Thomas, S.; Groeninckx, G. Micro- and Nanostructured Multiphase Polymer Blend Systems Phase Morphology and Interfaces; CRC Press Taylor & Francis Group: Boca Raton, FL, **2006**.
3. Lvov, Y. M.; Shchukin, D. G.; Mohwald, H.; Price, R. R. *ACS Nano.* **2008**, *2*(5), 814.
4. Du, M.; Guo, B.; Jia, D. *Polym. Int.* **2010**, *59*, 574.
5. Guimaraes, L.; Enyashin, A. N.; Seifert, G.; Duarte, H. A. *J. Phys. Chem. C* **2010**, *114*, 11358.
6. Liu, M.; Jia, Z.; Liu, F.; Jia, D.; Guo, B. *J. Colloid Interface Sci.* **2010**, *350*, 186.
7. Du, M.; Guo, B.; Jia, D. *Eur. Polym. J.* **2006**, *42*, 1362.
8. Liu, M.; Guo, B.; Du, M.; Chen, F.; Jia, D. *Polymer* **2009**, *50*, 3022.
9. Kongkhlang, T.; Reddy, K. R.; Kitano, T.; Nishu, T.; Tashiro, K. *Polym. J.* **2011**, *43*, 66.
10. Hu, Y.; Ye, L.; Zhao, X. *Polymer* **2006**, *47*, 2649.
11. Andrews, E. H.; Martin, G. E. *J. Mater. Sci.* **1973**, *8*, 1315.
12. Ning, N.; Yin, Q.; Luo, F.; Zhang, Q.; Du, R.; Fu, Q. *Polymer* **2007**, *48*, 7374.
13. Prashantha, K.; Lacrampe, M. F.; Krawczak, P. *Exp. Polym. Lett.* **2011**, *5*(4), 295.
14. Li, Y.; Shimizu, H. *Polymer* **2004**, *45*, 7381.
15. Yah, W. O.; Takahara, A.; Lvov, Y. M. *J. Am. Chem. Soc.* **2012**, *134*, 1853.
16. Yuan, P.; Southon, P. D.; Liu, Z.; Green, M. E. R.; Hook, J. M.; Antill, S. J.; Kepert, C. J. *J. Phys. Chem. C* **2008**, *112*, 15742.
17. Nayak, G. C.; Rajasekar, R.; Bose, S.; Das, C. K. *J. Nanotech.* **2009**, doi:10.1155/2009/759374.
18. Nayak, G. C.; Rajasekar, R.; Das, C. K. *J. Mater. Sci.* **2011**, *46*, 2050.
19. Nayak, G. C.; Rajasekar, R.; Das, C. K. *Compos. Part A* **2010**, *41*, 1662.
20. Ye, Y.; Chen, H.; Wu, J.; Ye, L. *Polymer* **2007**, *48*, 6426.
21. Liu, M.; Guo, B.; Du, M.; Cai, X.; Jia, D. *Nanotechnology* **2007**, *18*, 455703.
22. Bose, S.; Pramanik, N.; Das, C. K.; Ranjan, A.; Saxena, A. K. *Mater. Des.* **2010**, *31*, 1148.
23. Nayak, G. C.; Rajasekar, R.; Das, C. K. *J. Appl. Polym. Sci.* **2011**, *119*, 3574.
24. Bao, S. P.; Tjong, S. C. *Mater. Sci. Eng. A* **2008**, *485*, 508.
25. Gilman, J. W. *Appl. Clay Sci.* **1999**, *15*, 31.
26. Nayak, G. C.; Sahoo, S.; Das, S.; Karthikeyan, G.; Das, C. K.; Saxena, A. K.; Ranjan, A. *J. Appl. Polym. Sci.* **2012**, *124*, 629.
27. Dhibar, S.; Kar, P.; Khatua, B. B. *J. Appl. Polym. Sci.* **2012**, *125*, E601.